Volatility Studies on Gallium Chalcogenide Cubanes: Thermal Analysis and Determination of Sublimation Enthalpies

Edward G. Gillan,[1a] Simon G. Bott,[1b] and Andrew R. Barron*,[1a,c]

Department of Chemistry and Department of Mechanical Engineering and Materials Science, Rice University, Houston, Texas 77005, and Department of Chemistry, University of North Texas, Denton, Texas, 76203

Received September 20, 1996. Revised Manuscript Received December 31, 1996[⊗]

Volatility trends are established for a series of organometallic molecular solids with a cubane geometry and the general form $[(R)Ga(\mu_3\text{-}E)]_4$, where R = Me_3C (^{t}Bu), $EtMe_2C$, Et_2-MeC, or Et_3C and E = S, Se, or Te. While the temperature of volatilization, T_{20} defined as 20% mass loss from thermogravimetric analysis, was found to generally increase in a linear fashion with respect to increasing molecular mass, perturbations were observed that can be attributed to intermolecular ligand interactions. Sublimation enthalpies (ΔH_{sub}) for each cubane were calculated from thermogravimetric data, which show that the dependence of ΔH_{sub} on the degree of branching of the alkyl ligand appears to be more substantial than molecular mass effects alone. The C−H···H−C van der Waals interactions between alkyl substituents are estimated to account for more than 60% of the ΔH_{sub} in the organometallic cubane system $[(R)Ga(\mu_3\text{-}E)]_4$. Calculations based on the number of hydrogen atoms present in each alkyl yields an approximate value of ca. 4 kJ mol^{-1} for each C−H···H−C interactions. Using the TGA sublimation data, vapor pressures may be calculated for each of the cubane compounds over a wide range of temperatures. All new cubanes have been characterized by MS, NMR, IR, and TG/DTA. The molecular structures of $[(Et_3C)_2Ga(\mu\text{-}Cl)]_2$, $[(Et_3C)Ga$-$(\mu_3\text{-}S)]_4$, and $[(Et_3C)Ga(\mu_3\text{-}Se)]_4$ have been determined by X-ray crystallography.

Introduction

The commercial desirability for high-purity inorganic thin films grown at low cost, in simple deposition systems, has led to wide ranging research in the area of metal−organic chemical vapor deposition (MOCVD).[2] The basic requirement for the MOCVD process is that of a volatile precursor that decomposes under the appropriate conditions (thermal, photochemical, or plasma) to allow for deposition of the desired inorganic material on a substrate.[3] However, legislative and practical considerations also require that, if possible, the precursor have a low toxicity. One advantage of MOCVD, over the more traditional CVD, is that the precursors tend to decompose and consequently form films at temperatures lower than those of their corresponding inorganic (i.e., halides, hydrides, etc.) counterparts. This allows inorganic films to be deposited on a wider range of thermally sensitive substrates.[4] In an effort to improve stoichiometric control in the deposition of binary solids, single-source molecules have been synthesized which contain both constituents of the product film. One detriment to using these single-source precursor systems is that they are inherently larger and more massive than their analogous dual-source counterparts, e.g., $[Me_2Ga(\mu\text{-}As^tBu_2)]_2$ (M_w = 577.9 g mol^{-1}) versus $GaMe_3$ (M_w = 114.8 g mol^{-1}) and AsH_3 (M_w = 77.9 g mol^{-1}). Consequently, in the majority of cases they form as molecular solids at room temperature and are generally much less volatile.

Industrial MOCVD processes rely almost exclusively on gaseous and liquid precursors because of their ease of delivery and stoichiometric control. Systems where solid precursors are employed are undesirable due to the difficulty of maintaining a constant flux of source vapors over a nonequilibrium percolation (solid) process. Such nonbubbling processes are a function of surface area, a nonconstant variable with respect both to time and particle size.[5] However, there are cases where solid systems are being used commercially to deposit films, e.g., $InMe_3$ (mp = 88 °C). If solid precursors are used, they should have sufficient vapor pressure and mass transport at the desired temperature, preferably below 200 °C. This upper temperature limit is not dictated by chemical factors; rather, it is a limitation imposed by the stability of the mass flow controllers and pneumatic valves utilized in commercial deposition equip-

* To whom correspondence should be addressed.

⊗ Abstract published in *Advance ACS Abstracts,* February 15, 1997.

(1) (a) Department of Chemistry, Rice University. (b) Department of Chemistry, University of North Texas. (c) Department of Mechanical Engineering and Materials Science, Rice University.

(2) For background on thin-film processes, see: (a) *Thin Film Processes*; Vossen, J. L., Kern, W., Eds.; Academic Press: New York, 1978. (b) *Thin Film Processes II*; Vossen, J. L., Kern, W., Eds.; Academic Press: New York, 1978.

(3) For general background, see: (a) *CVD of Metals*; Kodas, T., Hampden-Smith, M., Eds.; VCH: New York, 1994. (b) *CVD of Non-Metals*; Rees, Jr., W. S., Ed.; VCH: New York, 1996.

(4) While researchers have commonly correlated thermally sensitive substrates with those of low melting points or phase transitions, it should be noted that in most practical applications, proclusion of doping redistribution and the stability of heterojunctions within the substrate are actually more prevalent issues that require low-temperature film growth.

(5) The requirements for solid MOCVD precursors has been outlined elsewhere; see: Barron, A. R.; Rees, Jr., W. S. *Adv. Mater. Opt. Electron.* **1993**, *2*, 271.

S0897-4756(96)00485-1 CCC: $14.00

ment.[6] Since the majority of metal−organic compounds reported in the literature do not meet this requirement, three general approaches have been used to overcome this difficulty: (a) development of new delivery systems, (b) increased volatility of existing compounds through chemical modification, and (c) synthesis of entirely new compounds.

Techniques such as spray pyrolysis[7] and aerosol CVD[3a,8] use a solvent-assisted approach where low-volatility solids are dissolved (or dispersed) in an inert, volatile liquid which is then misted into a heated deposition area, whereupon the carrier solvent dissipates leaving the precursor to decompose on (or near) the substrate. Chemical approaches toward increasing molecular volatility of known classes of compounds have focused on effects of the ligand(s), i.e., structure and geometry, substituents, and intermolecular interaction. One class of MOCVD precursor that has probably received the greatest attention in this regard is that of the group 2 metals, in particular barium.[5,9] Examples in this area include the use of fluorinated ligands,[10] sterically hindered ligands,[11] and inter- and intramolecular Lewis bases.[12,13] It is interesting to note that attempts to design volatile precursors through truly rational approaches have not, at the time of writing, met with commercial success. In part this is due to a lack of a detailed understanding in the factors that control the volatility of metal−organic compounds.[14]

We have recently reported the MOCVD growth of gallium sulfide (GaS) from the single-source precursor compound $[(^t\text{Bu})\text{Ga}(\mu_3\text{-S})]_4$.[15,16] These films have been found to be a suitable material for the electronic passivation of GaAs surfaces[17] and may be used as an insulating gate material in field effect transistors (FETs),[18] as well as a facet coating for 980 nm laser diodes.[19] While $[(^t\text{Bu})\text{Ga}(\mu_3\text{-S})]_4$ is oxidatively, hydrolytically, thermally, and photochemically stable and decomposes to give the desired material under standard operation conditions, there are a number of drawbacks with respect to its use in the commercialization of the GaS/GaAs FETISH[20] devices. First, $[(^t\text{Bu})\text{Ga}(\mu_3\text{-S})]_4$ is a sublimable solid that does not melt prior to decomposition and as such presents greater technical challenges to a process engineer than is generally encountered with liquid CVD sources. Second, $[(^t\text{Bu})\text{Ga}(\mu_3\text{-S})]_4$ rearranges to $[(^t\text{Bu})\text{Ga}(\mu_3\text{-S})]_7$ upon prolonged heating.[21] Since MOCVD using $[(^t\text{Bu})\text{Ga}(\mu_3\text{-S})]_7$ results in amorphous GaS being deposited,[16] any conversion of $[(^t\text{Bu})\text{Ga}(\mu_3\text{-S})]_4$ to $[(^t\text{Bu})\text{Ga}(\mu_3\text{-S})]_7$ during film growth will result in loss of crystallinity of the deposited film. Third, the large-scale synthesis of $[(^t\text{Bu})\text{Ga}(\mu_3\text{-S})]_4$ is complicated owing to the existence of multiple reaction products. To enable ready compatibility with present MOCVD deposition systems and commercial fabrication, it would be desirable to have an alternative Ga−S cubane precursor that is a liquid, does not undergo any rearrangement reactions, and can be prepared as a single product on a large scale.

Our initial search for an alternative precursor focused on the $[(\text{EtMe}_2\text{C})\text{Ga}(\mu_3\text{-S})]_4$ and $[(\text{Et}_2\text{MeC})\text{Ga}(\mu_3\text{-S})]_4$ cubane molecules.[22] While not perfect, $[(\text{EtMe}_2\text{C})\text{Ga}(\mu_3\text{-S})]_4$ offers significant advantages over the *tert*-butyl precursor: it melts to a liquid without decomposition,[23] it is chemically and thermally stable in the region bordered by the evaporation and transport temperatures, even after prolonged use, and the synthesis is reproducible and allows for a high level of purity. Unfortunately, the volatilities of both $[(\text{EtMe}_2\text{C})\text{Ga}(\mu_3\text{-S})]_4$ and $[(\text{Et}_2\text{MeC})\text{Ga}(\mu_3\text{-S})]_4$ are significantly lower that of $[(^t\text{Bu})\text{Ga}(\mu_3\text{-S})]_4$. In fact a preliminary analysis suggested that the temperature of volatilization was related to the molecular mass (eq 1). With the failure to develop

$$[(^t\text{Bu})\text{Ga}(\mu_3\text{-S})]_4 < [(\text{EtMe}_2\text{C})\text{Ga}(\mu_3\text{-S})]_4 < [(\text{Et}_2\text{MeC})\text{Ga}(\mu_3\text{-S})]_4 \quad (1)$$

(6) It must be stressed that while the achievement of an *optimum* vapor pressure for efficient utilization as an industrially practicable source providing high film growth rates (>10 Torr at 25 °C) is a worthy goal, the usable pressure regimes are those in which evaluation can be carried out on compounds which exhibit vapor pressures exceeding 1 Torr at 100 °C.

(7) See for example: (a) Pluym, T. C.; Kodas, T. T.; Wang, L.-M.; Glicksman, H. D. *J. Mater. Res.* **1995**, *10*, 1661. (b) Milosevic, O.; Jordovic, B.; Uskokovic, D. *Mater. Lett.* **1994**, *19*, 165. (c) Gonzalez-Carreno, T.; Morales, M. P.; Gracia, M.; Serna C. J. *Mater. Lett.* **1993**, *18*, 151.

(8) See for example: (a) Xu, C.; Hampden-Smith, M. J.; Kodas, T. T. *Chem. Mater.* **1995**, *7*, 1539. (b) Gysling, H. J.; Wernberg, A. A.; Blanton, T. N. *Chem. Mater.* **1992**, *4*, 900. (c) Wernberg, A. A.; Gysling, H. J. *Chem. Mater.* **1993**, *5*, 1056.

(9) Rees, Jr., W. S.; Barron, A. R. *Mater. Sci. Forum* **1993**, *137−138*, 473.

(10) See for example: (a) Purdy, A. P.; Berry, A. D.; Holm, R. T.; Fatemi, M.; Gaskill, D. K. *Inorg. Chem.* **1989**, *28*, 2799. (b) Thompson, S. C.; Cole-Hamilton, D. J.; Gilliland, D. D.; Hitchman M. L.; Barnes, J. C. *Adv. Mater. Opt. Electron.* **1992**, *1*, 81. (c) Belcher, R.; Cranley, C. R.; Majer, J. R.; Stephen W. I.; Uden, P. C. *Anal. Chim. Acta* **1972**, *60*, 109.

(11) See for example: (a) Burkley, D. J.; Hanusa, T. P.; Huffman, J. C. *Adv. Mater. Opt. Electron.* **1994**, *4*, 1. (b) Williams, R. A.; Tesh, K. F.; Hanusa, T. P. *J. Am. Chem. Soc.* **1991**, *113*, 4843. (c) Williams, R. A.; Hanusa, T. P.; Huffman, J. C. *Organometallics* **1990**, *9*, 1128. (d) Hanusa, T. P. *Polyhedron* **1990**, *9*, 1345. (e) Burns, C. J.; Andersen, R. A. *J. Organomet. Chem.* **1987**, *325*, 31.

(12) (a) Dickinson, P. H.; Geballe, T. H.; Sanjurjo, A.; Hildenbrand, D.; Craig, G.; Zisk, M.; Collman, J.; Banning S. A.; Sievers, R. E. *J. Appl. Phys.* **1989**, *66*, 444. (b) Fujinaga, T.; Kuwamoto, T.; Maurai, S. *Talanta* **1971**, *18*, 429. (c) Spek, A. L.; van der Sluis, P.; Timmer, K.; Meinema, H. A. *Acta Crystallogr. C* **1990**, *46*, 1741. (d) Gardiner, R.; Brown, D. W.; Kirlin, P. S.; Rheingold, A. L. *Chem. Mater.* **1991**, *3*, 1053. (e) Malandrino, G.; Richeson, D. S.; Marks, T. J.; DeGroot, D. C.; Schindler, J. L.; Kannewurf, C. R. *Appl. Phys. Lett.* **1991**, *58*, 182. (f) Matsuno, S.; Urchikawa, F.; Yoshizaki, K. *Jpn. J. Appl. Phys.* **1990**, *29L*, 947. (g) Zhao, J.; Marcy, H. O.; Tonge, L. M.; Wessels, B. W.; Marks, T. J.; Kannewurf, C. R. *Physica C* **1989**, *159*, 710. (h) Buriak, J. M.; Cheatham, L. K.; Gordon, R. G.; Graham, J. J.; Barron, A. R. *Eur. J. Solid State Inorg. Chem.* **1992**, *29*, 43. (i) Norman, J. A. T.; Pez, G. P. *J. Chem. Soc., Chem. Commun.* **1991**, 971.

(13) See for example: (a) Rees, Jr., W. S.; Caballero, C. R.; Hesse, W. *Angew. Chem.* **1992**, *104*, 786. (b) Rees, Jr., W. S.; Moreno, D. A. *J. Chem. Soc., Chem. Commun.* **1991**, 1759. (c) Rees, Jr., W. S.; Dippel K. A. In *Ultrastructure Processing of Ceramics, Glasses, Composites, Ordered Polymers, and Advanced Optical Materials, V*; Hench, L. L., West J. K., Ulrich, D. R., Eds.; Wiley and Sons: New York, 1992; p 327. (d) Rees, Jr., W. S.; Dippel K. A. *Org. Prepr. Proc. Intl.* **1992**, *24*, 531.

(14) Recent studies have tried to develop a rational approach to enhanced volatility for sodium alkoxides, $[\text{Na(OR)}]_4$, see: Samuels, J. A.; Folting, K.; Huffman, J. C.; Caulton, K. G. *Inorg. Chem.* **1995**, *7*, 929.

(15) MacInnes, A. N.; Power, M. B.; Barron, A. R. *Chem. Mater.* **1992**, *4*, 11.

(16) MacInnes, A. N.; Power, M. B.; Barron, A. R. *Chem. Mater.* **1993**, *5*, 1344.

(17) MacInnes, A. N.; Power, M. B.; Barron, A. R.; Jenkins, P. P.; Hepp, A. F. *Appl. Phys. Lett.* **1993**, *62*, 771.

(18) (a) Jenkins, P. P.; MacInnes, A. N.; Tabib-Azar, M.; Barron, A. R. *Science* **1994**, *263*, 1751. (b) Barron, A. R. *Mater. Res. Soc., Symp. Proc.* **1996**, *410*, 23.

(19) MacInnes, A. N.; Barron, A. R., unpublished results.

(20) FETISH = field effect transistor with insulating sulfide heterojunction.

(21) Power, M. B.; Ziller, J. W.; Barron, A. R. *Organometallics* **1992**, *11*, 2783.

(22) Power, M. B.; Barron, A. R.; Hnyk, D.; McMurdo, G.; Rankin, D. W. H. *Adv. Mater. Opt. Electron.* **1995**, *5*, 177.

(23) The melting point of $[(\text{Me}_2\text{EtC})\text{Ga}(\mu_3\text{-S})]_4$ (221 °C) is close to the temperature employed for the volatilization of $[(^t\text{Bu})\text{Ga}(\mu_3\text{-S})]_4$ during MOCVD growth (225 °C).

a volatile liquid cubane precursor, we embarked on an investigation of a series of gallium cubane compounds, $[(R)Ga(\mu_3\text{-}E)]_4$ (R = alkyl, E = S, Se, Te) to better understand the interplay between ligand interactions and molecular mass as they influence volatility and energy of sublimation.

The alkyl substituents examined in this study are structurally related to each other and vary only in the number of ethyl groups branching off the tertiary carbon which is bonded to a cage gallium atom: Me_3C (*tert*-butyl, ^{t}Bu, **I**), $EtMe_2C$ (*tert*-amyl, **II**), Et_2MeC (**III**), Et_3C

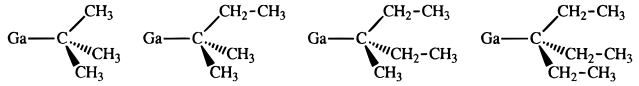

(I) (II) (III) (IV)

(**IV**). Initial studies[24] on the volatility of organometallic group 13 cubane molecules included $[(R)Al(\mu_3\text{-}E)]_4$ systems, but these were found to decompose in concert with sublimation which complicated their analysis and hence are not included herein.

Results and Discussion

A series of gallium cubane compounds of the general formula $[(R)Ga(\mu_3\text{-}E)]_4$ (**V**, where R = Me_3C, $EtMe_2C$, Et_2MeC, Et_3C, and E = S, Se, or Te) were synthesized

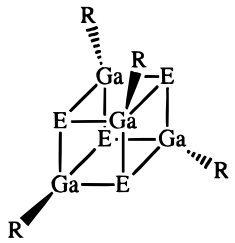

(**V**)

by adaptations of our previously described synthetic routes.[21,22,25,26] Except for the Et_3C derivatives, the chalcogenide cubanes are prepared from the direct reaction of the parent trialkyl with the elemental chalcogen (eq 2).

$$4GaR_3 + E\ (xs) \rightarrow [(R)Ga(\mu_3\text{-}E)]_4 + 4RE(E)_nR, \quad n = 1, 2, \ldots \quad (2)$$

Unfortunately, the trialkyl, $Ga(CEt_3)_3$, could not be prepared, presumably due to the steric bulk of the alkyl substituents. However, the dialkyl chloride, $[(Et_3C)_2Ga(\mu\text{-}Cl)]_2$, is readily synthesized (eq 3), and reaction of

$$2GaCl_3 + 4(Et_3C)MgCl \rightarrow [(Et_3C)_2Ga(\mu\text{-}Cl)]_2 + 4MgCl_2 \quad (3)$$

$$[(Et_3C)_2Ga(\mu\text{-}Cl)]_2 \xrightarrow[-NaCl]{+NaSH} \text{“}[(Et_3C)_2Ga(\mu\text{-}SH)]_n\text{”} \xrightarrow{-Et_3CH} [(Et_3C)Ga(\mu_3\text{-}S)]_4 \quad (4)$$

$[(Et_3C)_2Ga(\mu\text{-}Cl)]_2$ with NaSH results in the formation of the sulfide cubane, $[(Et_3C)Ga(\mu\text{-}S)]_4$, presumably via an unstable hydrosulfido compound (eq 4). The selenide and telluride cubanes were prepared (eq 5) by a variation of the method we have employed in the synthesis of indium chalcogenide cubanes[27] and presumably proceeds via a dimeric intermediate similar to $[R_2Ga(\mu\text{-}SR')]_2$ systems.[25]

$$2\,[(Et_3C)_2Ga(\mu\text{-}Cl)]_2 \xrightarrow[E = Se, Te]{+\text{“(MeE)Li”}} [(Et_3C)Ga(\mu_3\text{-}E)]_4 \quad (5)$$

Full details of the syntheses are given in the Experimental Section. The new compounds, $[(Et_2MeC)Ga(\mu_3\text{-}E)]_4$ (E = Se, Te) and $[(Et_3C)Ga(\mu_3\text{-}E)]_4$ (E = S, Se, Te), were characterized by NMR spectroscopy and mass spectrometry (see Experimental Section). In addition, the molecular structures of $[(Et_3C)Ga(\mu_3\text{-}S)]_4$, $[(Et_3C)Ga(\mu_3\text{-}Se)]_4$, and their synthon, $[(Et_3C)_2Ga(\mu\text{-}Cl)]_2$, were determined by X-ray crystallography; see below. Prior to use in thermogravimetric/differential thermal analyses (TG/DTA) the cubane compounds were purified by recystallization and used as polycrystalline solids.

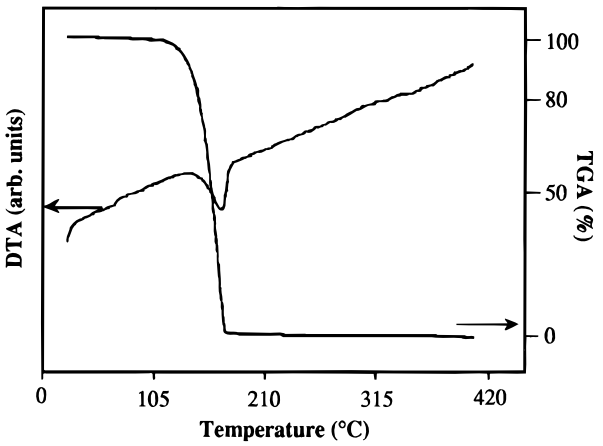

Figure 1. TG/DTA analysis of $[(EtMe_2C)Ga(\mu_3\text{-}Se)]_4$.

Relative Volatility of Gallium Chalcogenide Cubanes. Prior to a detailed analysis of volatility, it was important to first assess the volatility of each cubane over a wide temperature range to ensure that each compound could be sublimed intact without decomposition, i.e., eq 6. A simultaneous TG/DTA instrument was

$$[(R)Ga(\mu_3\text{-}E)]_4(solid) \rightarrow [(R)Ga(\mu_3\text{-}E)]_4(vapor) \quad (6)$$

used to monitor the sample mass losses and energetic events as a function of temperature. A typical TG/DTA result is shown in Figure 1. The uniform mass loss of $[(EtMe_2C)Ga(\mu_3\text{-}Se)]_4$ under vacuum is accompanied by a broad endothermic event characteristic of sublimation.[28] In some cubanes this thermal event is quite broad or is shifted near the end of the sublimation process, while in other cases melting occurs as evidenced by a sharp endotherm; therefore, the position of this thermal event was not a good indicator of relative cubane volatilities (sublimation temperature). To allow a direct comparison of the relative volatility of the various cubanes, a sublimation temperature was defined as the point when 20% mass loss had occurred (i.e., T_{20}),

(24) Gillan, E. G.; Bott, S. G.; Barron, A. R. *Mater. Res. Soc., Symp. Proc.* **1996**, *415*, 87.
(25) Power, M. B.; Ziller, J. W.; Tyler, A. N.; Barron, A. R. *Organometallics* **1992**, *11*, 1055.
(26) Harlan, C. J.; Gillan, E. G.; Bott, S. G.; Barron, A. R. *Organometallics* **1996**, *15*, 5479.
(27) Stoll, S. L.; Bott, S. G.; Barron, A. R. *J. Chem. Soc., Dalton Trans.*, in press.
(28) Turi, E. A.; Khanna, Y. P.; Taylor, T. J. In *A Guide to Materials Characterization and Analysis*; Sibilia, J. P., Ed.; VCH: New York, 1988; Chapter 9.

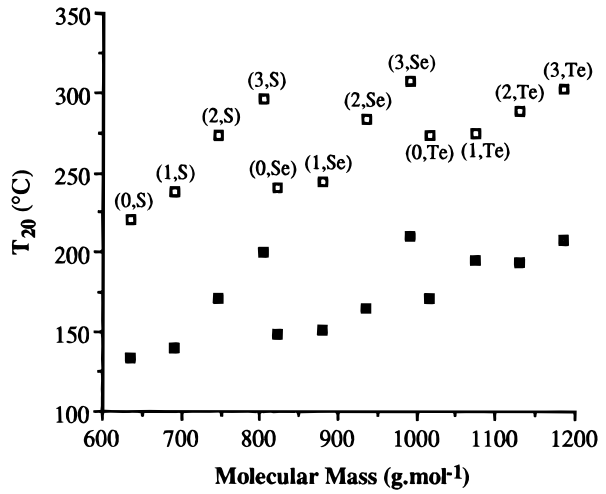

Figure 2. Plot of T_{20} volatility values derived from TGA data versus the molecular mass (M_w) of gallium chalcogenide cubanes, $[(R)Ga(\mu_3\text{-}E)]_4$, performed with atmospheric flow of an inert gas (□) and under dynamic vacuum, <0.2 Torr (■). For clarity atmospheric pressure data points are labeled with ($\#_{Et}$,E), where $\#_{Et}$ represents the number of ethyl groups in the alkyl substituent (i.e., $Me_3C = 0$, $EtMe_2C = 1$, $Et_2MeC = 2$, $Et_3C = 3$) and E is the chalcogenide. For example, $[(EtMe_2C)Ga(\mu_3\text{-}Se)]_4$ is represented by (1,Se).

and T_{20} values were determined for each compound under both flowing inert gas (nitrogen or argon) and dynamic vacuum (P < 0.2 Torr[29]) conditions. It should be noted that these T_{20} values represent the precursor temperatures required for these cubanes to be used in a CVD process. The effect of vacuum conditions over an atmospheric flow is that the T_{20} values are lower by nearly 100 °C. This proved most significant for the $[(R)Ga(\mu_3\text{-}Te)]_4$ cubanes, which have some of the highest volatilization temperatures and are the most thermally unstable.[30]

A plot of T_{20}, measured at atmospheric pressure and under dynamic vacuum, versus molecular mass (M_w) is shown Figure 2. The T_{20} values clearly increase with an increasing mass of the core, i.e., eq 7, and with

$$[(Me_3C)Ga(\mu_3\text{-}S)]_4 < [(Me_3C)Ga(\mu_3\text{-}Se)]_4 < [(Me_3C)Ga(\mu_3\text{-}Te)]_4 \quad (7)$$

$$[(Me_3C)Ga(\mu_3\text{-}S)]_4 < [(EtMe_2C)Ga(\mu_3\text{-}S)]_4 < [(Et_2MeC)Ga(\mu_3\text{-}S)]_4 < [(Et_3C)Ga(\mu_3\text{-}S)]_4 \quad (8)$$

increasing mass of the alkyl substituents (eq 8). However, these two trends are not collinear. Thus, while the T_{20} values for the *tert*-butyl derivatives, $[(Me_3C)Ga(\mu_3\text{-}E)]_4$, increase with an increased molecular mass in a near-linear manner, a significant deviation occurs for the more highly branched alkyl groups (i.e., $EtMe_2C < Et_2MeC < Et_3C$). In fact, although the molecular masses of $[(Et_3C)Ga(\mu_3\text{-}S)]_4$ (803 g mol^{-1}) and $[(Me_3C)Ga(\mu_3\text{-}Se)]_4$ (823 g mol^{-1}) are similar, their T_{20} values vary considerably: $[(Et_3C)Ga(\mu_3\text{-}S)]_4$ (T_{20} = 296 °C @ 760 Torr) versus $[(Me_3C)Ga(\mu_3\text{-}Se)]_4$ (T_{20} = 241 °C @ 760 Torr). A similar difference (ΔT_{20} = 52 °C) is observed under vacuum. The deviation from the *tert*-butyl values is also biggest for the sulfides, $[(R)Ga(\mu_3\text{-}S)]_4$, smallest for tellurides, $[(R)Ga(\mu_3\text{-}Te)]_4$.[31] Data on the tellurides, however, are complicated by their high air sensitivity and low thermal stability. Since near identical trends are observed for measurements made at both atmospheric pressure and dynamic vacuum, there is clearly an additional factor (other than molecular mass) that contributes to determining the volatility of the gallium chalcogenide cubanes.

Caulton and co-workers[14] have demonstrated in the case of sodium alkoxides, $[Na(OR)]_4$, fluorination of the alkyl substituents significantly increases the volatility, e.g., $[NaOC(CF_3)_3]_4$ (T_{sub} = 119 °C) is more volatile than $[NaOC(CH_3)_2(CF_3)]_4$ (T_{sub} = 177 °C). The rationale for this effect was proposed to be due to the lower intermolecular interactions for the fluorinated derivatives. In view of the foregoing and based on precedent in the volatilities of organic compounds,[32] we propose that the increases in the T_{20} values observed for the branched alkyl substituents are a consequence of the intermolecular interactions between alkyl groups. Two possible effects should be considered. First is the strength of intermolecular dispersion interactions, i.e., the potential number of C−H···H−C van der Waal interactions that can occur between molecules in the solid (or liquid) state. Second, we have previously observed in the solid-state structure of $[(EtMe_2C)Al(\mu_3\text{-}Se)]_4$ that the ethyl groups of the *tert*-amyl substituents on adjacent molecules are interlocked in a "lobster claw" geometry.[26] Therefore, the possibility of intertwining of the ligands must be considered. Clearly both effects are related; however, it would be desirable to express these effects in a quantitative (or at least semiquantitative) manner.

It is difficult to measure the exact number of C−H···H−C van der Waal interactions for each of the cubane molecules; however, a reasonable correlation is obtained by employing, as a correction to the data in Figure 2, the ratio of alkyl hydrogens in ligand R as compared to CMe_3 (eq 9). Using eq 9, values for n_H

$$n_H = \frac{\text{number of hydrogens in ligand R}}{\text{number of hydrogens in } CMe_3} \quad (9)$$

are as follows: $Me_3C = 1$, $EtMe_2C = 1.22$, $Et_2MeC = 1.44$, and $Et_3C = 1.67$. Figure 3 shows a plot of T_{20} values versus $M_w n_H$. We note that this is clearly a simplification (and approximation) of the problem since it assumes that all possible C−H groups are available for intermolecular interactions, and observation of space filling views of the cubane molecules from X-ray structures show that only "external" C−H's may be involved in intermolecular interactions. However, for the purposes of these discussions it appears a valid approximation since the resulting plot shown in Figure 3 follows a much more linear pattern than Figure 2, confirming that the extent of C−H···H−C van der Waal interactions is a contributing factor toward the degree of volatility of the gallium chalcogenide cubanes.

In an attempt at examine the effects of alkyl branching on volatility, the value n_C was defined the average number of carbons branching from the tertiary carbon

(29) Non Si unit. Torr = 1 mmHg = 133.322 Pa.

(30) Vacuum sublimation enables these less stable cubanes to be used as precursors in the MOCVD of GaTe films: Gillan, E. G.; Barron, A. R., submitted for publication.

(31) It should be noted that the contribution to molecular weight from the alkyl substituent is greatest for $[(Et_3C)Ga(\mu_3\text{-}S)]_4$ (49% of total) and least for $[(Me_3C)Ga(\mu_3\text{-}Te)]_4$ (22% of total).

(32) Israelachvili, J. N. *Intermolecular and Surface Forces*, 2nd ed.; Academic Press: New York, 1992; p 83.

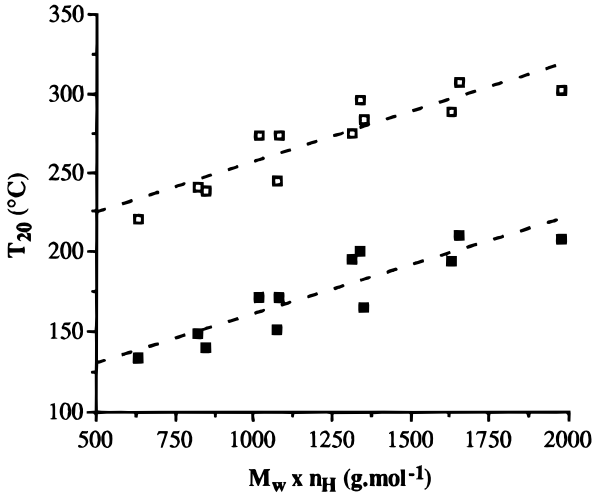

Figure 3. Plot of T_{20}, determined under atmospheric flow of an inert gas (□) and under dynamic vacuum (■), versus the molecular mass (M_w) of the gallium chalcogenide cubanes, [(R)-Ga(μ_3-E)]$_4$, weighted by the number alkyl hydrogens (n_H) on the cubane molecule.

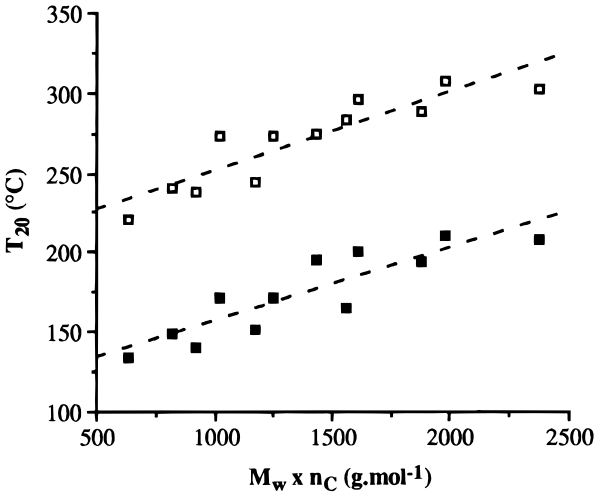

Figure 4. Plot of T_{20}, determined under atmospheric flow of an inert gas (□) and under dynamic vacuum (■), versus the molecular mass (M_w) of the gallium chalcogenide cubanes, [(R)-Ga(μ_3-E)]$_4$, weighted by the number of alkyl carbon branches (n_C, see text).

relative to Me_3C (eq 10). Using eq 10, values for n_C are

$$n_C = \frac{\text{number of nonquaternary carbons in ligand R}}{\text{number of nonquaternary carbons in } CMe_3} \quad (10)$$

as follows: $Me_3C = 1$, $EtMe_2C = 1.33$, $Et_2MeC = 1.67$, and $Et_3C = 2$. Figure 4 shows a plot of T_{20} data versus $M_w n_C$. The improved linearity of Figure 4 indicates that the deviations from linearity observed in Figure 2 may also be accounted for by considering increased intermolecular interactions from "intertwined" ethyl groups of the alkyl ligands.[26]

Determination of Sublimation Enthalpies (ΔH_{sub}) of Gallium Chalcogenide Cubanes. While the sublimation temperature of a molecular precursor is of practical interest for MOCVD deposition experiments, a far more quantitative measure of volatility for solids is the enthalpy of sublimation (ΔH_{sub}). The gallium cubane molecules offer an almost ideal system of study

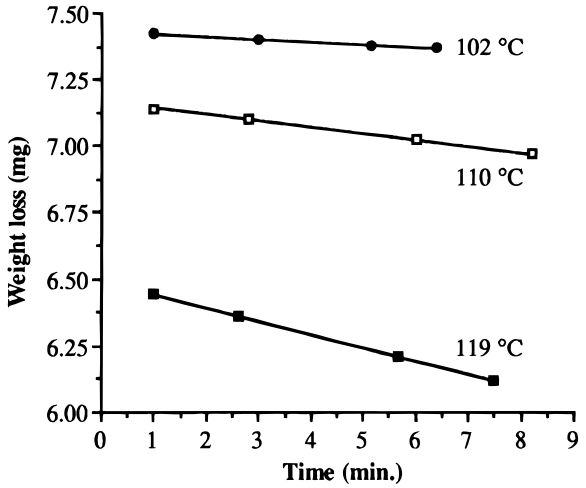

Figure 5. Plot of vacuum TGA results for [(Me$_3$C)Ga(μ_3-Se)]$_4$ performed at different isothermal steps.

since their molecular structures are similar (i.e., isostructural), they sublime without decomposition, and both the core mass (i.e., the chalcogen) and the intermolecular interactions (i.e., the alkyl substituent) may be varied in a systematic manner. We have therefore determined the ΔH_{sub} for each of the gallium chalcogenide cubane compounds described above.

Enthalpies of sublimation for molecular compounds have been determined through a variety of methods, most commonly from vapor pressure measurements using complex experimental systems, such as Knudsen effusion and temperature drop microcalorimetry.[33] More recently enthalpies of sublimation determinations have been accomplished by the direct measurement of enthalpy changes using differential scanning calorimetry (DSC).[34] While other thermal techniques, such as thermogravimetric analysis (TGA) have found use in molecular decomposition studies,[35] there have been relatively few studies reporting sublimation enthalpy determinations using TGA data. This is perhaps surprising since Ashcroft outlined a TGA method for ΔH_{sub} determination which was found to yield a high degree of accuracy and reproducibility.[36] We have employed this method to determine the enthalpy of sublimation (ΔH_{sub}) of the [(R)Ga(μ_3-E)]$_4$ cubanes described above.

An ideal sublimation process involves no compound decomposition and only results in a phase change (solid to gas) in the material (cf., eq 6). Since phase changes are thermodynamic processes following zero-order kinetics, the evaporation rate or rate of mass loss by sublimation (m_{sub}) is constant at a given temperature (eq 11). Thus m_{sub} values can be simply determined

$$\text{sublimation rate at temperature } T = \Delta[(R)Ga(\mu_3\text{-}E)]_4/\Delta t = m_{sub} \quad (11)$$

from the linear mass loss of the TGA data in isothermal regions. As an illustrative example, Figure 5 shows

(33) Hill, J. O.; Murray, J. P. *Rev. Inorg. Chem.* **1993**, *13*, 125.
(34) (a) Beech, G.; Lintonbon, R. M. *Thermochim. Acta* **1971**, *3*, 97. (b) Murry, J. P.; Cavell, K. J.; Hill, J. O. *Thermochim. Acta* **1980**, *36*, 97. (c) Torres-Gomez, L. A.; Barreiro-Rodriquez, G.; Galarza-Mondragon, A. *Thermochim. Acta* **1988**, *124*, 229.
(35) See for example: (a) Bukovec, N.; Bukovec, P.; Siftar, J. *Thermochim. Acta* **1980**, *35*, 85. (b) Slifirski, J.; Huchet, G.; Marty, A.; Teyssandier, F. *Chem. Mater.* **1995**, *7*, 622 and references therein.
(36) Ashcroft, S. J. *Thermochim. Acta* **1971**, *2*, 512.

Table 1. Thermodynamic Results on [(R)Ga(μ_3-E)]$_4$ Cubanes

compound	mol wt (g mol^{-1})	measd range (°C)	ΔH_{sub} (kJ mol^{-1})	ΔS_{sub} (J K^{-1} mol^{-1})	T_{sub}(calc) (°C)	T_{20}(vacuum) (°C)	vapor pressure @ 150 °C (Torr)
[(Me_3C)Ga(μ_3-S)]$_4$	635	94−107	110	300	94	134	22.75
[($EtMe_2C$)Ga(μ_3-S)]$_4$	691	96−109	124	330	102	140	18.89
[(Et_2MeC)Ga(μ_3-S)]$_4$	747	134−147	137	339	131	172	1.173
[(Et_3C)Ga(μ_3-S)]$_4$	803	159−171	149	333	175	201	0.018
[(Me_3C)Ga(μ_3-Se)]$_4$	823	102−115	119	305	116	149	3.668
[($EtMe_2C$)Ga(μ_3-Se)]$_4$	879	122−134	137	344	124	152	2.562
[(Et_2MeC)Ga(μ_3-Se)]$_4$	935	115−147	147	359	136	165	0.815
[(Et_3C)Ga(μ_3-Se)]$_4$	991	179−191	156	339	189	210	0.005
[(Me_3C)Ga(μ_3-Te)]$_4$	1017	118−149	131	315	143	172	0.374
[($EtMe_2C$)Ga(μ_3-Te)]$_4$	1074	143−159	140	325	157	195	0.109
[(Et_2MeC)Ga(μ_3-Te)]$_4$	1129	159−174	151	347	163	194	0.055
[(Et_3C)Ga(μ_3-Te)]$_4$	1185	171−183	156	342	184	208	0.007

data for the [(Me_3C)Ga(μ_3-Se)]$_4$ system under dynamic vacuum (0.2 Torr) and each isothermal data set can be closely fit to a linear relation ($R^2 > 0.99$). The linear slope, equal to m_{sub}, increases with increasing temperature as is expected from an endothermal phase change.

It is important to discuss at this point the various factors which must be controlled in order to obtain meaningful (useful) m_{sub} data from TGA data. First, the sublimation rate is independent of the amount of material used but may exhibit some dependence on the flow rate of an inert carrier gas, since this will affect the equilibrium concentration of the cubane in the vapor phase. While little variation was observed we decided that for consistency m_{sub} values should be derived from vacuum experiments only. Second, the surface area of the solid in a given experiment should remain approximately constant, otherwise the sublimation rate (i.e., mass time^{-1}) at different temperatures cannot be compared, since as the relative surface area of a given crystallite decreases during the experiment the apparent sublimation rate will also decrease. To minimize this problem, data were taken over a small temperature ranges (ca. 30 °C), and overall sublimation was kept low (ca. 25% mass loss representing a surface area change of less than 15%).[37] Third, the compound being analyzed must not decompose to any significant degree, because the mass changes due to decomposition will cause a reduction in the apparent m_{sub} value, producing erroneous results. With our simultaneous TG/DTA system it is possible to observe exothermic events if decomposition occurs; however, the clearest indication is shown by the mass loss versus time curves which are no longer linear but exhibit exponential decays characteristic of first- or second-order decomposition processes. None of the gallium cubanes studied here showed any decomposition, and all could be fully sublimed by 250 °C, leaving less than 5% residue.

The basis of analyzing isothermal TGA data involves using the Clausius−Clapeyron relation between vapor pressure (p) and temperature (T), eq 12,[38] where ΔH_{sub}

$$d(\ln p)/dT = \Delta H_{sub}/RT^2 \qquad (12)$$

is the enthalpy of sublimation and R is the gas constant (8.314 J K^{-1} mol^{-1}). Since m_{sub} data are obtained from TGA data, it is necessary to utilize the Langmuir equation (eq 13)[39] which provides an equality between

$$p = [2\pi RT/M_w]^{1/2} m_{sub} \qquad (13)$$

vapor pressure of a solid in vacuum with its sublimation rate. After integrating eq 12 in log form, substituting in eq 13, and consolidating the constants, one obtains the useful equality eq 14. Thus, the linear slope of a

$$\log(m_{sub}T^{1/2}) = \frac{-0.0522(\Delta H_{sub})}{T} + \left[\frac{0.0522(\Delta H_{sub})}{T_{sub}} - {}^1/_2\log\left(\frac{1306}{M_w}\right)\right] \qquad (14)$$

$\log(m_{sub}T^{1/2})$ versus $1/T$ plot yields ΔH_{sub}. In addition, the y intercept of such a plot provides a value for T_{sub}, the calculated sublimation temperature at the system pressure (0.2 Torr in our case). Table 1 lists calculated results for each cubane along with T_{20}(vac) values for comparison. Two volatile solids with known ΔH_{sub} values were examined to determine the accuracy of this approach. Hexamethylbenzene (Me_6C_6, M_w = 162 g mol^{-1}) and iron(III) acetylacetonate [Fe(acac)$_3$, M_w = 353 g mol^{-1}] yielded values of 80 kJ mol^{-1} (lit. 81.4 kJ mol^{-1})[40] and 118 kJ mol^{-1} (lit. 113.6 kJ mol^{-1}),[41] respectively. Repetition of the gallium cubane compounds allowed for an estimation of the reproducibility of this technique to be within 10%, consistent with previous reports.[33]

A plot of the sublimation enthalpies, determined for each of the gallium chalcogenide cubane compounds (see Table 1) versus the M_w of the compound is shown in Figure 6. Most striking is that the ΔH_{sub} values for all the cubanes demonstrate only a general trend with respect to the cubane's mass. However, there are clear trends within each chalcogen set, e.g., a linear trend is observed for [(Me_3C)Ga(μ_3-S)]$_4$, [($EtMe_2C$)Ga(μ_3-S)]$_4$, [(Et_2MeC)Ga(μ_3-S]$_4$, and [(Et_3C)Ga(μ_3-S)]$_4$, as well as for the selenium and tellurium homologues. In each case the ΔH_{sub} increases in a linear fashion with increasing alkyl group branching and mass. There are also clear nearly linear relationships between different chalcogenide cubanes with the same alkyl group, e.g., a linear trend is observed for [(Me_3C)Ga(μ_3-S)]$_4$, [(Me_3C)Ga(μ_3-Se)]$_4$, [(Me_3C)Ga(μ_3-Te)]$_4$. As with the results obtained for T_{20} measurements, any significant molecular mass effect may be ruled out after considering two pairs of

(37) In experiments where significant surface area changes occurred the values of m_{sub} deviated significantly from linearity on a log(m_{sub}) versus 1/T plot.

(38) Castellan, G. W. *Physical Chemistry*, 2nd ed.; Addison-Wesley: Menlo Park, CA, 1983; pp 268−269.

(39) Langmuir, I. *Phys. Rev. (second series)* **1913**, *2*, 329.

(40) Sabbah, R.; Tabet, D.; Belaadi, S. *Thermochim. Acta* **1994**, *247*, 193.

(41) Sachinidis, J.; Hill, J. O. *Thermochim. Acta* **1980**, *35*, 59.

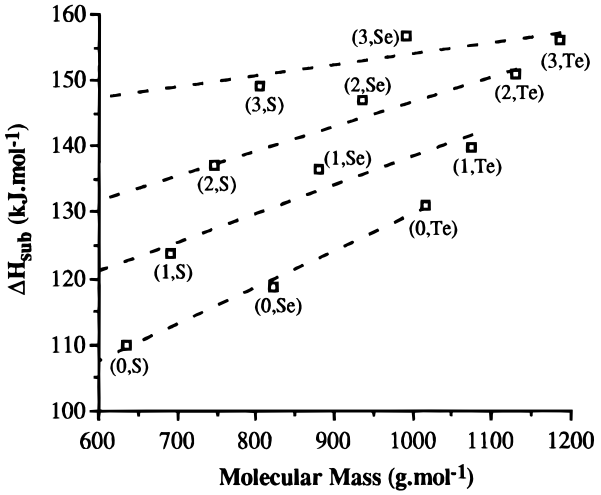

Figure 6. Graph of experimentally determined ΔH_{sub} values plotted against cubane molecular mass. The dashed lines represent a linear extrapolation of the data for a given R group back to zero mass. Data points are labled with ($\#_{Et}$,E), where $\#_{Et}$ represents the number of ethyl groups in the alkyl substituent (i.e., $Me_3C = 0$, $EtMe_2C = 1$, $Et_2MeC = 2$, $Et_3C = 3$) and E is the chalcogenide. For example, $[(EtMe_2C)Ga(\mu_3\text{-}Se)]_4$ is represented by (1,Se).

Table 2. Extrapolation of ΔH_{sub} Data to $M_w = 0$

alkyl group	ΔH_{sub} at $M_w = 0$ (kJ mol^{-1})	percent of total ΔH_{sub} (%)	$\Delta H_{sub} \times 1/c_H$ (kJ mol^{-1})
CMe_3	74	56−67	4.1
$CEtMe_2$	97	69−78	4.4
CEt_2Me	111	74−81	4.3
CEt_3	136	87−91	4.5

cubanes which are closest in mass, i.e., $[(Et_3C)Ga(\mu_3\text{-}S)]_4$ (M_w = 803 g mol^{-1}) versus $[(Me_3C)Ga(\mu_3\text{-}Se)]_4$ (M_w = 823 g mol^{-1}) and $[(Et_3C)Ga(\mu_3\text{-}Se)]_4$ (M_w = 991 g mol^{-1}) versus $[(Me_3C)Ga(\mu_3\text{-}Te)]_4$ (M_w = 1017 g mol^{-1}). While within each of these pairs their molecular masses are similar, they exhibit the most disparate ΔH_{sub} values.

The entropy of sublimation is readily calculated from the ΔH_{sub} and the calculated T_{sub} data in Table 1 (eq 15). The range observed for all the gallium chalcogenide

$$\Delta S_{sub} = \Delta H_{sub}/T_{sub} \qquad (15)$$

cubane compounds [ΔS_{sub} = 330 ± 20 J K^{-1} mol^{-1}] is slightly larger than values reported for organic compounds (100−200 J K^{-1} mol^{-1}), as would be expected for a transformation giving translational and internal degrees of freedom. Interestingly, for any particular chalcogenide, i.e., $[(R)Ga(\mu_3\text{-}S)]_4$, the lowest ΔS_{sub} are observed for the Me_3C derivatives, and the largest ΔS_{sub} for the Et_2MeC derivatives; see Table 1. This is in line with the relative increase in the modes of freedom for the alkyl groups in the absence of crystal packing forces.

An approximate measure of the alkyl group's influence on the total value for the ΔH_{sub} may be determined by extrapolating each set of data for a given R group back to zero mass (see dashed lines in Figure 6). These values are listed in Table 2 along with their percentage of the total ΔH_{sub} from Table 1. The percentage is highest for compounds with the Et_3C ligand and lowest for those with the Me_3C ligand. However, the important point to make here is that the intermolecular alkyl interactions contribute between 50% and 90% of the

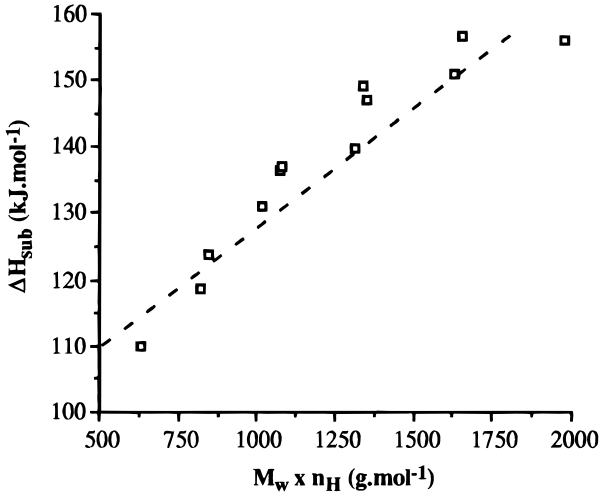

Figure 7. Plot of ΔH_{sub} values against a M_w weighted by the number of alkyl hydrogens (n_H) on the cubane molecules, $[(R)Ga(\mu_3\text{-}E)]_4$ (see text).

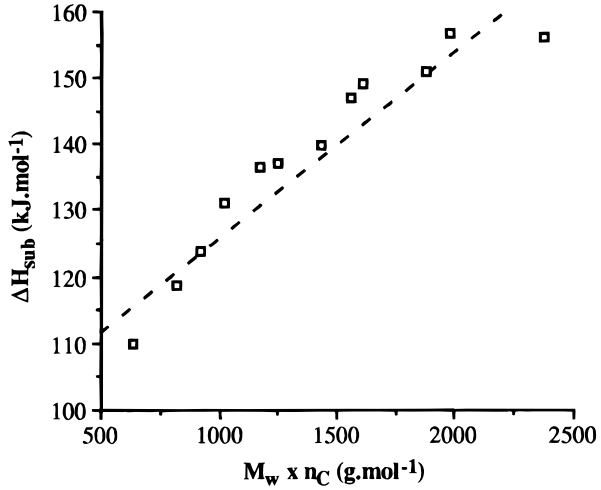

Figure 8. Plot of ΔH_{sub} values against a M_w weighted by the number of alkyl carbon branches (n_C) on the cubane molecules, $[(R)Ga(\mu_3\text{-}E)]_4$ (see text).

total sublimation energy. If one considers that this contribution is due to C−H···H−C van der Waals bonding, then the average strength of intermolecular dispersion interactions, or C−H···H−C van der Waals interaction energy, can be calculated. This bond energy is presented in the last column of Table 2 where c_H is the number of intermolecular hydrogen−hydrogen interactions, equal to half the number of total hydrogens on the cubane. The calculated values are within the range 4.1−4.5 kJ mol^{-1}. This is consistent with literature values determined for weak van der Waals interactions in hydrocarbons.[32] As was seen above for the T_{20} volatility data, plotting ΔH_{sub} versus either $M_w n_H$ (Figure 7) or $M_w n_C$ (Figure 8) again results in a much more linear relationship, and reinforces the importance of hydrogen contacts/ligand interactions on sublimation enthalpy.

Theoretical calculations on dispersion forces between straight chain alkanes predict that the enthalpy of sublimation increases by approximately 6.9 kJ mol^{-1} for each additional CH_2 unit in the alkane chain. The measured energies agree closely with theory.[41] If this theory is applied to the cubane systems studied here (with a CH_3 group worth 9.8 kJ mol^{-1} and a CH_2 group worth 6.9 kJ mol^{-1}), one calculates ΔH_{sub} of 118, 145,

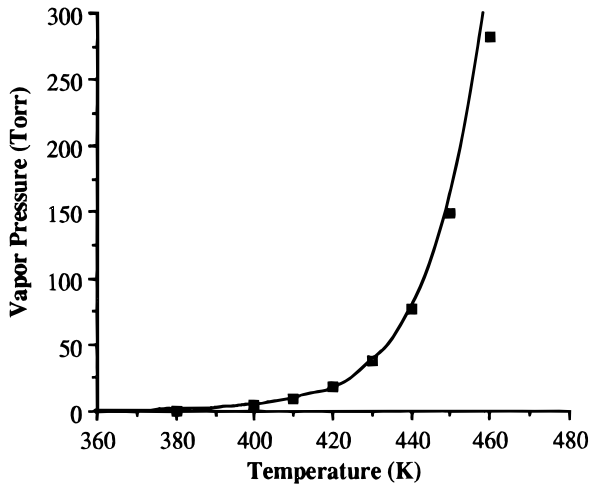

Figure 9. Plot of calculated vapor pressure (Torr) against temperature (K) for $[(Me_3C)Ga(\mu_3\text{-}S)]_4$ [$p = (3.0980 \times 10^{-13})10^{(0.0326)T}$, $R = 0.997$].

173, and 200 kJ mol^{-1} for Me_3C, $EtMe_2C$, Et_2MeC, and Et_3C, respectively. Since this dispersion relations strictly hold true for straight-chain alkyls, it is not surprising that the observed values in Table 2 are only ca. 65% of the calculated ones since chain branching limits the extent of alkyl−alkyl intermolecular interactions.

Indirect Determination of Vapor Pressures for Gallium−Chalcogenide Cubanes. While the sublimation temperature is an important parameter to determine the suitability of a potential precursor compounds for MOCVD, it is often preferable to express a compound's volatility in terms of its vapor pressure. However, while it is relatively straightforward to determine the vapor pressure of a liquid or gas, measurement of solids is difficult (e.g., use of the isoteniscopic method),[42] and few laboratories are equipped to perform such experiments. Given that TGA apparatus are increasingly accessible, it would therefore be desirable to have a simple method for vapor pressure determination that can be accomplished on a TGA.

Substitution of eq 13 into eq 14 allows for the calculation of the vapor pressure (p) of the cubane compounds as a function of temperature (T). For example, Figure 9 shows the calculated temperature dependence of the vapor pressure for $[(Me_3C)Ga(\mu_3\text{-}S)]_4$. The calculated vapor pressures for each of the gallium chalcogenide cubane compounds at 150 °C are given in Table 1. We note that literature values for vapor pressure measurements often vary significantly depending on the method and/or experimentalist.[41] We have found the TGA approach to show reasonable agreement with previous measurements. For example, the value calculated for $Fe(acac)_3$ (e.g., 2.75 Torr @ 113 °C) is slightly higher than that measured directly by the isoteniscopic method (0.53 Torr @ 113 °C); however, it should be noted that measurements using the sublimation bulb method obtained values much lower (8×10^{-3} Torr @ 113 °C).[41] On the basis of these results, we propose that this TGA method offers a suitable alternative to conventional (direct) measurements of vapor pressure.

Structural Studies. The molecular structures of $[(Et_3C)_2Ga(\mu\text{-}Cl)]_2$, $[(Et_3C)Ga(\mu_3\text{-}S)]_4$, and $[(Et_3C)Ga(\mu_3\text{-}Se)]_4$ have been determined by X-ray crystallography. Selected bond lengths and angles are shown in Tables 3 for $[(Et_3C)_2Ga(\mu\text{-}Cl)]_2$ and 4 for $[(Et_3C)Ga(\mu_3\text{-}S)]_4$ and $[(Et_3C)Ga(\mu_3\text{-}Se)]_4$.

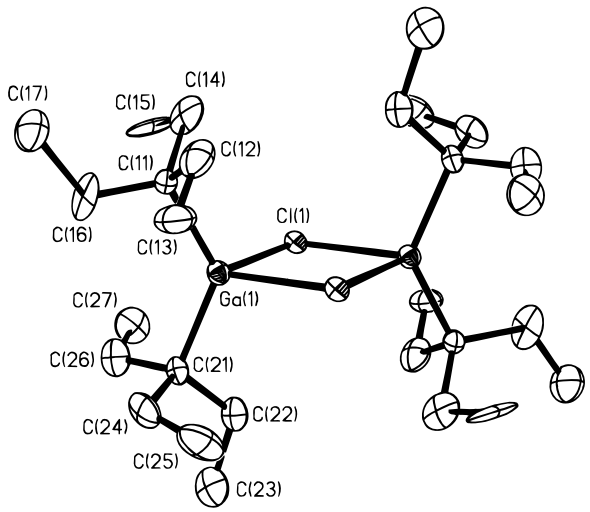

Figure 10. Molecular structure of $[(Et_3C)_2Ga(\mu\text{-}Cl)]_2$. Thermal ellipsoids are drawn at the 30% level, and hydrogen atoms are omitted for clarity.

Table 3. Selected Bond Lengths (Å) and Angles (deg) for $[(Et_3C)_2Ga(\mu\text{-}Cl)]_2$

Ga(1)−Cl(1)	2.438(2)	Ga(1)−Cl(1a)	2.432(2)
Ga(1)−C(11)	2.022(9)	Ga(1)−C(21)	2.020(9)
Cl(1)−Ga(1)−Cl(1a)	82.26(6)	Cl(1)−Ga(1)−C(11)	110.6(3)
Cl(1)−Ga(1)−C(11)	107.3(3)	C(11)−Ga(1)−C(21)	129.3(4)
C(11)−Ga(1)−Cl(1a)	108.8(3)	C(21)−Ga(1)−Cl(1a)	108.4(2)
Ga(1)−Cl(1)−Ga(1a)	97.74(8)		

Table 4. Selected Bond Lengths (Å) and Angles (deg) for $[(Et_3C)Ga(\mu_3\text{-}S)]_4$ and $[(Et_3C)Ga(\mu_3\text{-}Se)]_4$

	$[(Et_3C)Ga(\mu_3\text{-}S)]_4$	$[(Et_3C)Ga(\mu_3\text{-}Se)]_4$
Ga(1)−E(1)	2.349(9)	2.483(2)
Ga(1)−E(2)	2.346(9)	2.481(2)
Ga(1)−C(11)	2.14(3)	2.01(1)
Ga(2)−E(1)	2.36(1)	2.483(3)
Ga(2)−C(21)	2.102(7)	1.97(3)
E(1)−Ga(1)−E(2)	95.9(3)	97.56(7)
E(1)−Ga(1)−C(11)	121(1)	120.2(6)
E(1)−Ga(1)−E(1a)	96.1(2)	97.79(6)
E(2)−Ga(1)−C(11)	121.4(7)	119.5(5)
E(2)−Ga(1)−E(1a)	95.7(2)	97.70(8)
C(11)−Ga(1)−E(1a)	120.5(9)	119.2(5)
E(1)−Ga(2)−C(21)	121.1(3)	119.63(9)
E(1)−Ga(2)−E(1a)	95.8(3)	97.7(1)
Ga(1)−E(1)−Ga(2)	83.8(3)	81.67(9)
Ga(1)−E(1)−Ga(1a)	83.7(7)	81.80(8)
Ga(1)−E(2)−Ga(1a)	84.0(4)	81.81(9)

The molecular structure of $[(Et_3C)_2Ga(\mu\text{-}Cl)]_2$ is shown in Figure 10. As is common for group 13 metal chloride compounds the structure consists of a centrosymmetric chloride bridged dimer. The Ga(1)−Cl(1) bond distance [2.438(2) Å] is similar to the values observed previously for similar compounds [2.343(4)−2.460(6) Å],[43] and the chloride bridge is symmetrical within experimental error.

(42) See for example: Arm, H.; Daeniker, H.; Schaller, R. *Helv. Chim. Acta* **1966**, *48*, 1772.

(43) (a) Beachley, Jr., O. T.; Hallock, R. B.; Zhang, H. M.; Atwood, J. L. *Organometallics* **1985**, *4*, 1675. (b) Atwood, D. A.; Cowley, A. H.; Jones, R. A.; Mardones, M. A.; Atwood, J. L.; Bott, S. G. *J. Coord. Chem.* **1992**, *25*, 233. (c) Neumüller, B.; Gahlmann, F. *Chem. Ber.* **1993**, *126*, 1579. (d) Petrie, M. A.; Power, P. P.; Rasika, H. V.; Ruhlandt-Senge, K.; Waggoner, K. M.; Wehmschulte, R. J. *Organometallics* **1993**, *12*, 1086.

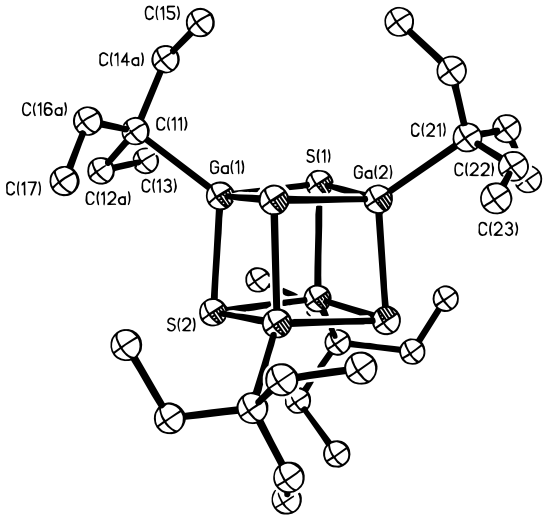

Figure 11. Molecular structure of $[(Et_3C)Ga(\mu_3\text{-}S)]_4$. Thermal ellipsoids are drawn at the 30% level. Only one of the positions for the disorder of the ethyl groups is shown. Hydrogen atoms are omitted for clarity.

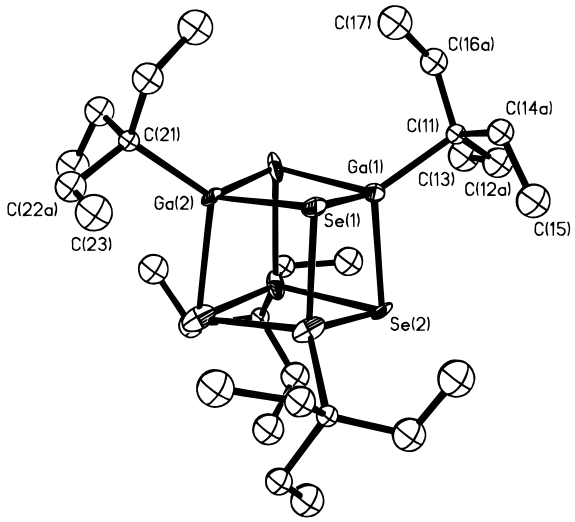

Figure 12. Molecular structure of $[(Et_3C)Ga(\mu_3\text{-}Se)]_4$. Thermal ellipsoids are drawn at the 25% level. Only one of the positions for the disorder of the ethyl groups is shown. Hydrogen atoms are omitted for clarity.

The molecular structures of $[(Et_3C)Ga(\mu_3\text{-}S)]_4$ and $[(Et_3C)Ga(\mu_3\text{-}Se)]_4$ are shown in Figures 11 and 12, respectively. The Ga−E bond distances, as well as the E−Ga−E and Ga−E−Ga angles, in $[(Et_3C)Ga(\mu_3\text{-}S)]_4$ and $[(Et_3C)Ga(\mu_3\text{-}Se)]_4$ are almost identical with that observed for their *tert*-butyl and *tert*-amyl analogues in both the solid state and vapor phase,[22,25,26,44,45] consistent with the highly stable nature of the Ga_4E_4 cores. The organic groups in $[(Et_3C)Ga(\mu_3\text{-}E)]_4$ show a site occupancy disorder similar to what we have previously observed in $[(Me_2EtC)Al(\mu_3\text{-}S)]_4$.[26] While the α- and γ-carbon atoms have a fixed position, the β-carbon atoms exhibit rotation about the Ga−C vector, resulting in a reversal of the conformation of the ethyl substituent (see Figure 13). The rotation of the *tert*-amyl group about the Ga−C bond and the fixed position of the γ-carbon

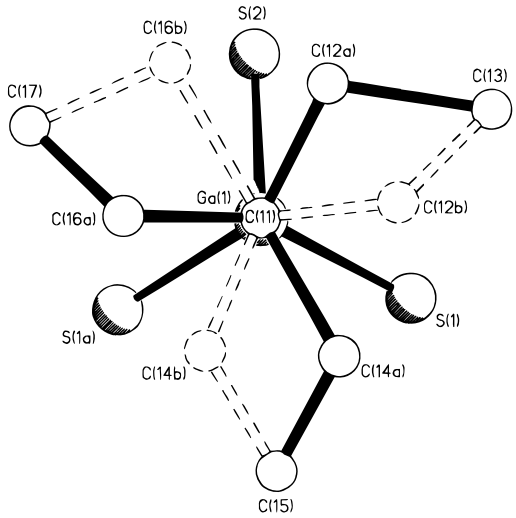

Figure 13. Partial coordination sphere of Ga(1) in $[(Et_3C)\text{-}Ga(\mu_3\text{-}S)]_4$ viewed along the C(11)−Ga(1) vector, showing the disordered ligand. Hydrogens have been omitted for clarity.

suggest that its conformation is defined by the crystal packing of the γ-carbon, i.e., $Ga-C(CH_2CH_3)_3$. Similar disorder has been reported for PEt_3 complexes,[46] and we are finding that this form of static disorder is common for short yet "floppy" ligands.[26,47]

It is not readily apparent why there exists disorder of the CEt_3 groups in the structures of $[(Et_3C)Ga(\mu_3\text{-}E)]_4$ (E = S and Se) but not in $[(Et_3C)_2Ga(\mu\text{-}Cl)]_2$. However, concideration of space-filling diagrams, and interligand distances, suggests that the disordered pseudo C_3 propeller-like ligand geometry observed in $[(Et_3C)Ga(\mu_3\text{-}E)]_4$ (i.e., Figure 13) would result in significant van der Waal repulsion between the two CEt_3 groups on each gallium, as well as those across the Ga_2Cl_2 core. Thus, the CEt_3 groups in $[(Et_3C)_2Ga(\mu\text{-}Cl)]_2$ adopt a geometry (see Figure 10) that minimizes H···H interactions and result in the interlocking of the $C-CH_2-CH_3$ groups. In the cubane structures the CEt_3 are at a sufficient distance apart [C(11)···C(21) = 6.59 Å] as compared to those in $[(Et_3C)_2Ga(\mu\text{-}Cl)]_2$ [C(11)···C(21) = 3.65 Å, C(11)···C(21a) = 5.39 Å] that free movement of the ethyl groups occurs and disorder results. Similar effects has been observed for the "disorder-prone" *tert*-amyl group, $CEtMe_2$.[26]

Conclusion

We have determined the sublimation temperature (T_{20}) and enthalpy of sublimation (ΔH_{sub}) for a series of gallium chalcogenide cubane molecules, $[(R)Ga(\mu_3\text{-}E)]_4$. While the volatility of the *tert*-butyl cubanes decreases with increased molecular mass (i.e., eq 7), there is significant deviation from this trend with regard to the other ligands studied. The deviation increases in the

(44) Cleaver, W. M.; Späth, M.; Hoyk, D.; McMurdo, G.; Power, M. B.; Stuke, M.; Rankin, D. W. H.; Barron, A. R. *Organometallics* **1995**, *14*, 690.

(45) Power M. B.; Barron, A. R. *J. Chem. Soc., Chem. Commun.* **1991**, 1315.

(46) See for example: (a) Weaver, D. L. *Inorg. Chem.* **1970**, *9*, 2250. (b) Hitchcock, P. B.; Lappert, M. L.; Pye, P. L.; Thomas, S. *J. Chem. Soc., Dalton Trans.* **1979**, 1929. (c) Bianchini, C.; Ghilardi, C. A.; Meli, A.; Midollini, S.; Orlandini, A. *Organometallics* **1982**, *1*, 778. (d) Overbosch, P.; van Koten, G.; Grove, D. M.; Spek, A. L.; Duisenberg, A. J. M. *Inorg. Chem.* **1982**, *9*, 21. (e) Burgess, K.; Johnson, B. J. G.; Kaner, D. A.; Lewis, J.; Raithby, P. R.; Azman, S. N.; Syed-Mustaffa, B. *J. Chem. Soc., Chem. Commun.* **1983**, 455. (f) Usón, R.; Fornién, J.; Navarro, R.; Usón, M.; Garcia, M. P.; Welch, A. J. *J. Chem. Soc., Dalton Trans.* **1984**, 345. (g) Peng, W.-J.; Bleeke, J. R. *Organometallics* **1987**, *6*, 1576.

(47) Aitken, C. L.; Barron, A. R. *J. Chem. Crystallogr.* **1996**, *26*, 297.

order $EtMe_2C < Et_2MeC < Et_3C$. We have proposed that the apparent lower volatilities observed for these ligands (versus *tert*-butyl) can be attributed to intermolecular ligand interactions. Previous studies of the sublimation enthalpies for organic and organometallic systems also showed a strong dependence on the nature of the ligand, rather than on the molecular mass of the compounds. For example, only a slight variation is observed in ΔH_{sub} for Al(acac)$_3$ ($M_w = 324$ g mol^{-1}), Fe(acac)$_3$ ($M_w = 353$ g mol^{-1}), and Zn(acac)$_2$ ($M_w = 264$ g mol^{-1}),[41] whereas a strong dependence was found of ΔH_{sub} on degree of ligand fluorination in copper(II) β-diketonate complexes independent of molecular mass.[48] There are also various reports on organic systems where structure not molecular mass is found to dominate. The enthalpy of vaporization of substituted benzenes is linearly related to the number of methyl groups,[40] and the sublimation energies of branched glycols have been used to determine values of O−H···O hydrogen bond energies.[49]

We have proposed that for the gallium chalcogenide cubanes the dispersion forces between the molecules may be modeled by a combination of the number of possible intermolecular C−H···H−C van der Waals interactions, and the degree of branching of the alkyl ligand. Simple, but effective, approximations (corrections) for each of these effects have been proposed based upon the ratio of alkyl hydrogens in ligand R as compared to *tert*-butyl (n_H) and the average number of carbons branching from the tertiary carbon relative to *tert*-butyl (n_C). While it is possible to estimate the average strength of intermolecular dispersion interactions to be within the range 4.1−4.5 kJ mol^{-1} per C−H···H−C van der Waals interaction, it is difficult to quantitatively estimate the effect of ligands intertwining. However, we have previously reported a direct observation of the effect of ligand geometry through a comparison of the relative volatility of [(Me$_3$C)In(μ_3-Se)]$_4$ and [(^{n}Bu)In(μ_3-Se)]$_4$.[27] Decomposition of [(^{n}Bu)In(μ_3-Se)]$_4$ occurs prior to sublimation (240 °C), despite the compound having a molecular mass identical with [(Me$_3$C)In(μ_3-Se)]$_4$ ($T_{sub} = 151$ °C @ 0.2 Torr).

It is clear from the foregoing that our understanding of "how to make more volatile organometallic compounds" is still in its infancy. However, aided by modern thermogravimetric techniques and the development of basic thermochemical−intermolecular relationships, we hope that the future will allow for a rational approach to precursor design to be developed.

Experimental Section

The synthesis and characterization of many of the [(R)Ga(μ_3-E)]$_4$ cubanes used in this study have been described previously.[22,25,26] (Et$_3$C)MgCl and Ga(CEt$_2$Me)$_3$ were prepared by literature procedures.[22,50] All reactions were performed under inert atmosphere using Schlenk techniques. Selenium (Aldrich, 99.8%) and tellurium powder (Aesar, 99.8%) and 3-ethyl-3-pentanol (Aldrich, 98%) were used as received. ^{1}H and ^{13}C NMR was performed on a Bruker AC 250 MHz spectrometer, IR spectroscopy was taken with a Perkin-Elmer spectrometer, and electron impact mass spectra were obtained using a MAT 250 analyzer.

[(Et$_2$MeC)Ga(μ_3-Se)]$_4$. Ga(CEt$_2$Me)$_3$ (8.9 g, 27.4 mmol) and excess black selenium powder (8.6 g, 0.109 mol) were combined with 150 mL of dry toluene and refluxed overnight. The yellow solution was filtered, and its volume was reduced. This solution was set aside in the freezer (−23 °C) overnight to yield a pale yellow polycrystalline solid, yield 80%, mp 213−215 °C. MS (EI, %) *m/z* 938 (M$^+$, 20), 850 (M$^+$ − C$_6$H$_{13}$, 100), 766 (M$^+$ − 2C$_6$H$_{13}$, 25), 680 (M$^+$ − 3C$_6$H$_{13}$, 15), 620 (M$^+$ − 2C$_6$H$_{13}$ − GaSe, 20), 596 (M$^+$ − 4C$_6$H$_{13}$, 20), 535 (M$^+$ − 3C$_6$H$_{13}$ − GaSe, 20). IR (Nujol mull, cm^{-1}) 1328 (s), 1289 (s), 1261 (s), 1178 (m), 1150 (s), 1094 (w), 1050 (w), 1000 (w), 967 (w), 800 (s), 744 (s), 511 (m), 489 (m). ^{1}H NMR (C$_6$D$_6$) δ 1.59 [4H, m, J(H−H) = 7.0 Hz, *C*H$_2$CH$_3$], 1.10 (3H, s, CC*H*$_3$), 1.04 [6H, t, J(H−H) = 7.3 Hz, CH$_2$C*H*$_3$]. ^{13}C NMR (C$_6$D$_6$) δ 38.2 (Ga−*C*), 31.9 (*C*H$_2$CH$_3$), 22.5 (C*C*H$_3$), 11.4 (CH$_2$*C*H$_3$).

[(Et$_2$MeC)Ga(μ_3-Te)]$_4$. Ga(CEt$_2$Me)$_3$ (5.3 g, 16.4 mmol) and excess black tellurium powder (7.3 g, 57.2 mmol) were combined with 150 mL of dry toluene, stirred 1 day, and then refluxed overnight. The yellowish-orange solution was filtered and its volume was reduced. This solution was set aside in the freezer (−23 °C) overnight to yield a light orange polycrystalline solid, yield 75%, mp >270 °C (dec). MS (EI, %) *m/z* 1130 (M$^+$, 20), 1047 (M$^+$ − C$_6$H$_{13}$, 100), 962 (M$^+$ − 2C$_6$H$_{13}$, 25), 877 (M$^+$ − 3C$_6$H$_{13}$, 20), 793 (M$^+$ − 4C$_6$H$_{13}$, 45), 765 (M$^+$ − 2C$_6$H$_{13}$ − GaTe, 15), 679 (M$^+$ − 3C$_6$H$_{13}$ − GaTe, 20), 595 (M$^+$ − 4C$_6$H$_{13}$ − GaTe, 30). IR (Nujol mull, cm^{-1}) 1329 (w), 1260 (s), 1144 (m), 1096 (s), 1021 (s), 870 (w), 801 (s), 671 (m). ^{1}H NMR (C$_6$D$_6$) δ 1.40 [4H, q, J(H−H) = 7.6 Hz, *C*H$_2$CH$_3$], 1.01 [6H, t, J(H−H) = 7.5 Hz, CH$_2$C*H*$_3$], 0.85 (3H, s, CC*H*$_3$). ^{13}C NMR (C$_6$D$_6$) δ 32.2 (*C*H$_2$CH$_3$), 26.2 (Ga−*C*), 22.9 (C*C*H$_3$), 10.8 (CH$_2$*C*H$_3$).

[(Et$_3$C)$_2$Ga(μ-Cl)]$_2$. To GaCl$_3$ (16.2 g, 92.0 mmol) dissolved in 500 mL of dry pentane was added 0.55 M (Et$_3$C)MgCl in diethyl ether (65.7 g, 0.184 mol). After the addition was complete, the solution was refluxed for 3 h and then let stir overnight. The solution was filtered and pumped dry. The crude product was recrystallized from hexane prior to use. Large clear blocks were grown from a toluene solution, yield ca. 90%, mp 91−93 °C. MS (EI, %) *m/z* 302 (M$^+$, 50), 267 (M$^+$ − Cl, 100), 168 (M$^+$ − Cl − C$_7$H$_{15}$, 100), 100 (C$_7$H$_{16}$, 100). IR (Nujol mull, cm^{-1}) 1341 (w), 1326 (m), 1282 (w), 1259 (s), 1174 (m), 1136 (w), 1069 (w), 1059 (w), 1033 (m), 1018 (s), 905 (w), 841 (w), 797 (s), 741 (s), 669 (w), 580 (m), 500 (s). ^{1}H NMR (C$_6$D$_6$) δ 1.71 [2H, q, J(H−H) = 7.5 Hz, *C*H$_2$CH$_3$], 0.81 [3H, t, J(H−H) = 7.4 Hz, CH$_2$C*H*$_3$]. ^{13}C NMR (C$_6$D$_6$) δ 27.7 (*C*H$_2$CH$_3$), 11.2 (CH$_2$*C*H$_3$).

[(Et$_3$C)Ga(μ_3-S)]$_4$. [(Et$_3$C)$_2$Ga(μ-Cl)]$_2$ (1.0 g, 3.3 mmol) and NaSH (0.186 g, 3.3 mmol) were combined with dry toluene (150 mL) and refluxed overnight. The solution was filtered, its volume was reduced, and then it was set aside in the freezer. Clear blocks grew out of solution, yield ca. 50%, mp >270 °C (sub). MS (EI, %) *m/z* 804 (M$^+$, 20), 705 (M$^+$ − C$_7$H$_{15}$, 100), 606 (M$^+$ − 2C$_7$H$_{15}$, 60), 508 (M$^+$ − 3C$_7$H$_{15}$, 60), 405 (M$^+$ − 4C$_7$H$_{15}$, 50), 307 (M$^+$ − 4C$_7$H$_{15}$ − GaS), 271 (M$^+$ − C$_7$H$_{15}$ − GaS$_2$, 20). IR (Nujol mull, cm^{-1}) 1322 (s), 1300 (m), 1261 (s), 1144 (s), 1067 (w), 1017 (w), 850 (w), 800 (s), 739 (s), 694 (w), 489 (s). ^{1}H NMR (C$_6$D$_6$) δ 1.71 [2H, q, J(H−H) = 7.5 Hz, *C*H$_2$CH$_3$], 1.04 [3H, t, J(H−H) = 7.5 Hz, CH$_2$C*H*$_3$]. ^{13}C NMR (C$_6$D$_6$) δ 28.5 (*C*H$_2$CH$_3$), 11.1 (CH$_2$*C*H$_3$).

[(Et$_3$C)Ga(μ_3-Se)]$_4$. MeLi (3.4 mmol, 0.5 M in diethyl ether) diluted in 150 mL of toluene was combined with excess black selenium powder (0.4 g, 5.1 mmol) and stirred for 2 h. To this solution was added [(Et$_3$C)$_2$Ga(μ-Cl)]$_2$ (1.0 g, 3.3 mmol) dissolved in dry toluene (100 mL). The reaction mixture was then refluxed overnight. The resulting solution was filtered, and its volume was reduced. The clear yellow filtrate was set aside in the freezer and yellow blocks grew out of solution, yield ca. 60%, mp >270 °C (sub). MS (EI, %) *m/z* 991 (M$^+$, 15), 892 (M$^+$ − C$_7$H$_{15}$, 100), 794 (M$^+$ − 2C$_7$H$_{15}$, 20), 695 (M$^+$ − 3C$_7$H$_{15}$, 15), 644 (M$^+$ − 2C$_7$H$_{15}$ − GaSe, 10), 596 (M$^+$ − 4C$_7$H$_{15}$, 20), 546 (M$^+$ − 3C$_7$H$_{15}$ − GaSe, 20), 448 (M$^+$ − 4C$_7$H$_{15}$ − GaSe, 10). IR (Nujol mull, cm^{-1}) 1322 (s), 1294 (m), 1261 (m), 1150 (s), 1067 (w), 1017 (m), 844 (w), 800 (s), 733 (m), 694 (w), 489-(w). ^{1}H NMR (C$_6$D$_6$) δ 1.65 [2H, q, J(H−H) = 7.5 Hz, *C*H$_2$-

(48) Ribeiro da Silva, M. A. V.; Ferrao, M. L. C. C. H. *J. Chem. Thermodynamics* **1994**, *26*, 315.
(49) Font, J.; Muntasell, J. *Mater. Res. Bull.* **1994**, *29*, 1091.
(50) *Introduction to Organic Laboratory Techniques*; Pajia, D. L.; Lampman, G. M.; Kritz, J. R.; Saunders College Publishing: New York, 1982; pp 176, 222.

Table 5. Summary of X-ray Diffraction Data

compound	$[(Et_3C)_2Ga(\mu\text{-}Cl)]_2$	$[(Et_3C)Ga(\mu_3\text{-}S)]_4$	$[(Et_3C)Ga(\mu_3\text{-}Se)]_4$
empir formula	$C_{28}H_{60}Cl_2Ga_2$	$C_{28}H_{60}Ga_4S_4$	$C_{28}H_{60}Ga_4Se_4$
cryst size, mm	0.17 × 0.24 × 0.28	0.09 × 0.09 × 0.09	0.07 × 0.07 × 0.07
cryst system	orthorhombic	rhombohedral	rhombohedral
space group	*Pbca*	*R*3	*R*3
a, Å	13.124(1)	17.266(1)	17.460(1)
b, Å	14.907(1)		
c, Å	16.888(1)	10.5732(8)	10.6910(8)
V, Å^3	3304.0(4)	2729.7(4)	2822.5(5)
Z	4	3	3
D(calcd), g/cm^3	1.220	1.467	1.750
μ, mm^{-1}	1.802	3.158	6.672
radiation	Mo Kα (λ = 0.710 73 Å) graphite monochromator		
temp, K	298	298	298
2θ range, deg	2.0−44.0	2.0−44.0	3.0−44.0
no. collected	2320	2208	2292
no. ind	2320	1392	766
no. obsd	995 ($\|F_o\| > 6.0\sigma\|F_o\|$)	699 ($\|F_o\| > 5.0\sigma\|F_o\|$)	439 ($\|F_o\| > 6.0\sigma\|F_o\|$)
weighting scheme	$w^{-1} = \sigma^2(\|F_o\|) + 0.04(\|F_o\|)^2$	$w^{-1} = \sigma^2(\|F_o\|) + 0.04(\|F_o\|)^2$	$w^{-1} = \sigma^2(\|F_o\|)$
R	0.0398	0.0715	0.0273
R_w	0.0422	0.0829	0.0296
largest diff peak, e Å^{-3}	0.43	0.78	0.11

CH_3], 1.04 [3H, t, *J*(H−H) = 7.3 Hz, CH_2CH_3]. ^{13}C NMR (C_6D_6) δ 28.8 (CH_2CH_3), 10.9 (CH_2CH_3).

[(Et$_3$C)Ga(μ_3-Te)]$_4$. MeLi (3.4 mmol, 0.5 M in diethyl ether) diluted in 100 mL of toluene was combined with excess black selenium powder (0.6 g, 4.7 mmol) and stirred for 2 h. To this solution was added $[(Et_3C)_2Ga(\mu\text{-}Cl)]_2$ (1.0 g, 3.3 mmol) dissolved in dry toluene (25 mL). The reaction mixture was then refluxed for 1 day. The resulting solution was filtered, and its volume was reduced. The clear yellow filtrate was set aside in the freezer, and yellow crystals grew out of solution, yield 50%, mp >270 °C (dec). MS (EI, %) *m*/*z* 1188 (M^+, 15), 1089 ($M^+ - C_7H_{15}$, 100), 990 ($M^+ - 2C_7H_{15}$, 30), 890 ($M^+ - 3C_7H_{15}$, 15), 792 ($M^+ - 4C_7H_{15}$, 30), 694 ($5M^+ - 3C_7H_{15}$ − GaTe, 15), 594 ($M^+ - 4C_7H_{15}$ − GaTe, 15). IR (Nujol mull, cm^{-1}) 1321 (m), 1293 (m), 1152 (w), 1144 (s), 1094 (m), 1065 (w), 919 (w), 842 (m), 488 (m). ^{1}H NMR (C_6D_6) δ 1.43 [2H, q, *J*(H−H) = 7.4 Hz, CH_2CH_3], 1.02 [3H, t, *J*(H−H) = 7.5 Hz, CH_2CH_3]. ^{13}C NMR (C_6D_6) δ 29.9 (CH_2CH_3), 10.6 (CH_2CH_3).

Volatility Studies. The purified polycrystalline cubanes were analyzed for volatility and thermal events on a thermogravimetric analyzer (Seiko TG/DTA 200). Typically 5−10 mg of sample were measured with heating rates of 5 °C min^{-1} up to 400 °C under either a 200−300 mL min^{-1} inert (N_2 or Ar) gas flow or a 0.2 Torr dynamic vacuum (Welch DuoSeal pump). Vacuum runs were also performed under isothermal conditions at different temperatures over a small range (<30 °C). Isothermal mass loss was monitored over 10 min before moving to the next temperature plateau. In all cases studied here the mass loss at a given temperature was linear. The slope of each mass drop was measured and used to calculate sublimation enthalpies as discussed in the text. The validity of this method was verified with hexamethylbenzene and Fe(acac)$_3$ sublimation standards. It is important to note that while small amounts (<10%) of involatile impurities will not interfere with the ΔH_{sub} analysis, competitively volatile impurities will produce higher apparent sublimation rates.

Crystallographic Studies. Crystals of compounds $[(Et_3C)_2Ga(\mu\text{-}Cl)]_2$, $[(Et_3C)Ga(\mu_3\text{-}S)]_4$, and $[(Et_3C)Ga(\mu_3\text{-}Se)]_4$ were sealed in a glass capillary under argon and mounted on the goniometer of an Enraf-Nonius CAD-4 automated diffractometer. Data collection and cell determinations were performed in a manner previously described.[51] The structures were solved by using either SHELXS-86[52] for $[(Et_3C)Ga(\mu_3\text{-}S)]_4$ and $[(Et_3C)Ga(\mu_3\text{-}Se)]_4$, or Patterson, $[(Et_3C)_2Ga(\mu\text{-}Cl)]_2$, and difference Fourier maps using *MolEN*.[53] Site disorder of the β-carbon atoms was observed for the Et_3C groups in both $[(Et_3C)Ga(\mu_3\text{-}S)]_4$ and $[(Et_3C)Ga(\mu_3\text{-}Se)]_4$. This disorder could be easily modeled for the selenide; however, for the sulfide the model had to be restrained for the unique Et_3C group. and the disorder could not be resolved for this group on the 3-fold axis. Hydrogen atoms were included with fixed thermal parameters and constrained to "ride" upon the appropriate atoms [*d*(C−H) = 0.95 Å]. A summary of cell parameters, data collection, and structure solution is given in Table 5. Scattering factors were taken from ref 54.

Acknowledgment. Financial support for this work is provided by the Office of Naval Research, the National Science Foundation, and the Robert A. Welch Foundation. The assistance of Dr. Terry Marriot with mass spectroscopic measurements is gratefully acknowledged.

Supporting Information Available: Full listings of bond length and angles, anisotropic thermal parameters, and hydrogen atom parameters (15 pages); tables of calculated and observed structure factors (25 pages). Ordering information is given on any current masthead page.

CM960485J

(51) Mason, M. R.; Smith, J. M.; Bott, S. G.; Barron, A. R. *J. Am. Chem. Soc.* **1993**, *115*, 4971.
(52) Sheldrick, G. M. *Acta Crystallogr., A* **1990**, *46*, 467.
(53) Enraf-Nonius, *MolEN, An Interactive Structure Solution Procedure*; Enraf-Nonius: Delft, The Netherlands, 1990.
(54) *International Tables for X-ray Crystallography*; Kynoch Press: Birmingham, UK, 1974; Vol. IV, pp 99, 149.